NPL REPORT DQL-RD001

Characterisation of two new ionisation chamber types for use in reference electron dosimetry in the UK

Julia A D Pearce

September 2004

September 2004

CHARACTERISATION OF TWO NEW IONISATION CHAMBER TYPES FOR USE IN REFERENCE ELECTRON DOSIMETRY IN THE UK

Julia A D Pearce

Quality of Life Division
National Physical Laboratory
Teddington
Middlesex
United Kingdom
TW11 0LW

ABSTRACT

The IPEM Code of Practice (IPEM 2003) for electron dosimetry for radiotherapy beams recommends design requirements for parallel-plate ionisation chambers used to determine the absorbed dose to water in an electron beam. The Classic Markus design has been found not to meet these requirements. The Advanced Markus and the Exradin A10 ionisation chambers have been designed to rectify the problems associated with the Classic Markus ionisation chamber.

The response of one Exradin A10 and three Advanced Markus ionisation chambers was investigated. Absorbed dose to water calibration factors were derived at the National Physical Laboratory (NPL) for each ionisation chamber at seven electron energies in the range 4 to 19 MeV. Investigations were carried out into chamber settling, polarity effects, ion recombination and the chamber perturbation. The response of the ionisation chambers in a clinical beam was also investigated.

In general all three Advanced Markus ionisation chambers showed the same energy response. For the three Advanced Markus and one Exradin A10 ionisation chamber investigated the magnitude of the polarity effect was typically 5% at an energy of 4 MeV. There was discrepancy between the polarity measurements made at the NPL and in the clinic. Until further measurements are made the recommendation of this study is that these chambers are not suitable for use for reference dosimetry in electron beams.

ISSN 1744-0637

National Physical Laboratory
Queens Road, Teddington, Middlesex, UK, TW11 0LW

We gratefully acknowledge the financial support of the UK Department of Trade and Industry (National Measurement System Policy Unit)

Approved on behalf of the Managing Director, NPL
by Dr Martyn Sené, Director for Quality of Life Division

CONTENTS

TABLES

FIGURES

APPENDICES

1 INTRODUCTION AND OBJECTIVES

A very common method of radiation dosimetry is based on the measurement of the ionisation produced in a small mass of air. Measurements are made using air filled ionisation chambers, which are the most widely used dosemeters in standards laboratories and for therapy dose-rate clinical applications in hospitals. A well-designed air ionisation chamber has good long-term stability, enables precise measurements and can be read out in real time via a calibrated electrometer. These attributes make them the standard instrument of choice for clinical dosimetry measurements. An ionisation chamber typically consists of a thin (less than 1 mm) wall of graphite surrounding a very small (of the order of 0.5 cm^3) volume of air.

A schematic view of an air ionisation chamber with geometry suitable for electron dosimetry is shown in figure 1, Klevenhagen (1985). The chamber is used in a water phantom and placed in an electron beam. Electrons enter the sensitive volume of the chamber and produce ion pairs. A polarising voltage is applied across the plates of the chamber, which produces an electric field, enabling the ions to be collected. A measurement of the charge collected by the collecting electrode via a calibrated electrometer, combined with the chamber calibration factor can be used to determine the absorbed dose to water for that particular electron beam.

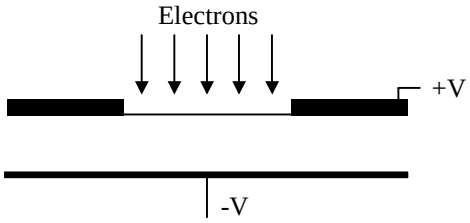

Figure 1. Schematic view of an ionisation chamber for electron dosimetry

The accurate determination of absorbed dose to water is crucial to the success of radiotherapy for the purpose of curing cancer. If the dose delivered to a patient is too small then a few cancerous cells may survive leading to a recurrence of the cancer. If the dose delivered is too large then healthy tissue may also be damaged. For example, optimal treatment of some head and neck tumours requires that the dose delivered should be within only a few percent of that prescribed. The large errors in patient positioning mean that it is crucial for all other errors to be as small as is possible. Accurate dosimetry is essential to improve patient survival rates.

The IPEM Code of Practice (IPEM 2003) for electron dosimetry for radiotherapy beams lists designated ionisation chambers to determine absorbed dose to water under reference conditions in an electron beam. At present only two parallel-plate chambers are recommended in the Code of Practice, the NACP-02 chamber manufactured by Scanditronix, and the PTW 34001 'Roos' chamber. These chambers fulfil certain requirements in the Code of Practice such as the magnitude of corrections for the polarity effect, the chamber perturbation and long-term stability of the chamber response.

The response of two new parallel-plate ionisation chamber types was characterised for electron beam radiotherapy: the Advanced Markus chamber, type 34045, manufactured by PTW-Freiburg, and the Exradin A10 chamber manufactured by Standard Imaging. Strontium-90 check source measurements corrected for decay were used to investigate the

ionisation chambers' stability over a period of time, while continuous current measurements enabled the settling time of the chambers to be determined. A full calibration of each chamber made it possible to examine perturbation effects, variations in the polarity effect with energy, and also the correction required due to recombination of ion pairs in the chamber. Radiographs and manufacturers' drawings permitted the chamber construction to be studied. It was then possible to determine whether or not the performance of the Advanced Markus chamber type and the Exradin A10 chamber fulfilled the requirements laid down by the IPEM Code of Practice (IPEM 2003) so that these chambers could in future be recommended for reference electron dosimetry.

2 BACKGROUND AND MOTIVATION

For an ionisation chamber to be recommended as a designated chamber for use for absolute dosimetry in electron beams it must satisfy the requirements described in the IPEM Code of Practice (IPEM 2003). These requirements, in the case of a parallel-plate chamber, are summarised in table A1 in the Appendix and described in more detail below.

A parallel-plate ionisation chamber should be designed for measurements in water. The human body is comprised of mostly water and it is the dose to water that the chamber is used to measure. The chamber construction should also be as homogenous and water equivalent as possible so that both mass stopping powers and linear scattering powers are similar to those of water. The walls should be made of a material with water-like properties. The air cavity must be vented to allow rapid equilibrium with the pressure and temperature of the surroundings.

It is possible to minimise in-scattering perturbation effects when using a parallel-plate chamber. This is achieved by ensuring that the chamber cavity is flat. For the cavity to be considered flat the ratio of the cavity diameter to the cavity depth should be of the order of ten. The cavity height should have a maximum of 2 mm and a guard ring should surround the collecting electrode. A guard ring is essential to the precise operation of a chamber. It serves two purposes, as explained in ICRU Report 35: the guard ring should be wide enough so that the lines of force from the electrical collecting field are perpendicular to the plane of the high voltage electrode and the collecting electrode over the entire area of the collecting electrode. It should also be wide enough so that electrons entering the cylindrical periphery of the flat chamber do not produce a significant number of ions in the collecting region.

The guard ring must have a width of at least 1.5 times the cavity height. Under these conditions the contribution of electrons entering through the side walls is negligible. This enables the effective point of measurement to be taken as being at the centre of the front surface of the air cavity.

To reduce the influence of radial non-uniformities of the electron beam profile the diameter of the collecting electrode should be less than 20 mm. The thickness of the front window should also be less than 1 mm to enable measurements at shallow depths. This is particularly important for use in low energy electron beams where the depth dose curve in water is changing rapidly. The use of a parallel-plate chamber with a very thin front window and well-defined reference point enables accurate determination of the depth at which the maximum dose occurs.

The polarity effect is an important parameter in determining whether an ionisation chamber is suitable for reference dosimetry in electron beams. It is the difference in chamber readings obtained in the same irradiation conditions but taken with positive and negative polarising voltages. In electron dosimetry the polarity effect is often caused by the capture of some of the primary electrons by the collecting electrode of the ionisation chamber, Klevenhagen (1985). The IPEM Code of Practice (IPEM 2003) recommends that the magnitude of this effect is less than 1%.

An ionisation chamber reading must have a correction applied for the incomplete collection of charge due to ion recombination. There are two types of ion recombination that may occur. Initial, or intratrack, recombination where the positive ions and negative ions that form in the same charged particle track meet and recombine is independent of dose and dose-rate. General, or intertrack, recombination when ions from different tracks meet on their way to the collecting electrode does depend on dose per pulse. The amount of general recombination that will occur depends on the number of ions created per unit volume.

The IPEMB Code of Practice (IPEMB 1996) for electron dosimetry for radiotherapy beams initially recommended the Classic Markus chamber, type 23343, as a designated chamber for use in electron beams. (The desirable properties of parallel-plate chambers in the IPEMB Code of Practice (IPEMB 1996) are the same as those properties now recommended in the IPEM Code of Practice (IPEM 2003), also given in IAEA (1996).) After initially including the Classic Markus chamber in the IPEMB Code of Practice (IPEMB 1996), it was later found by McEwen *et al* (2001) and others that this chamber did not meet all of the requirements of a parallel-plate chamber for reference dosimetry.

The main characteristics of the Classic Markus ionisation chamber are shown in table 1, IAEA (1996).

Materials	Window thickness	Electrode spacing (mm)	Collecting electrode diameter (mm)	Guard ring width (mm)
Graphited polyethylene foil window Graphited polystyrene collector PMMA body, PMMA cap	102 mg cm^{-2} 0.9 mm (incl. cap)	2	5.3	0.2

Table 1. Characteristics of the Classic Markus type ionisation chamber

The ratio of the Classic Markus chamber cavity diameter to cavity depth is approximately three. This is much less than the recommended value of ten so the chamber cavity cannot be considered flat. The guard ring has an exceptionally small width, of only 0.2 mm. The guard ring of the Classic Markus chamber is only 0.1 times the cavity height so the contribution to the fluence of electrons entering through the side walls is not negligible. As a result the effective point of measurement of this chamber type is about 0.5 mm behind the front surface of the air cavity. Further details of the work done to investigate this effect can be found in Roos *et al* (2000).

A schematic diagram of the Classic Markus chamber design is shown in figure 2 (Roos *et al* (2000)), showing the high-voltage electrode (HV), collecting electrode (C), and guard ring

(G). It can be seen that the HV plate is top hat shaped. This leads to a distorted electric field at the edge of the collecting volume. The very small width of the guard ring can also be clearly seen.

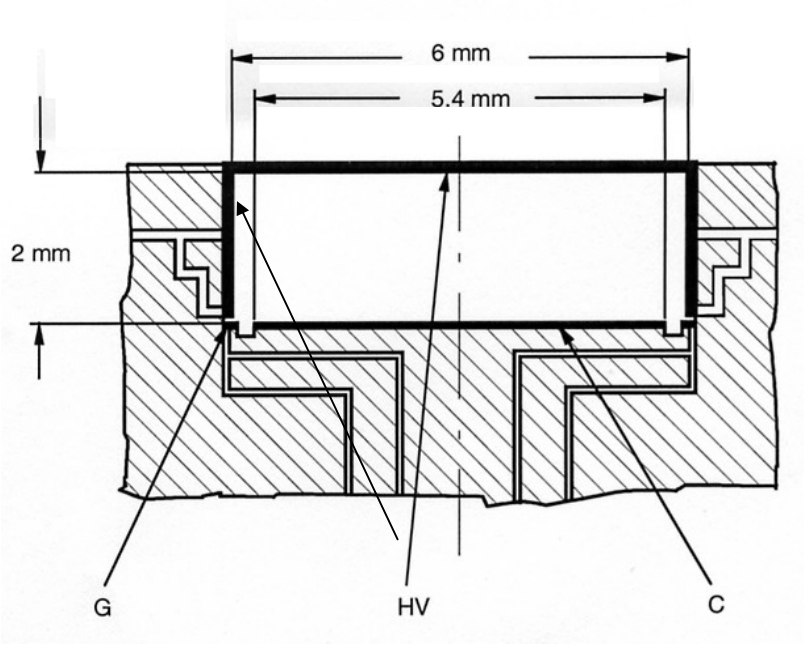

Figure 2. Design features of the Classic Markus chamber

It is believed that a well-designed, well-guarded parallel-plate ionisation chamber should have a zero perturbation correction. There are two components that contribute to the perturbation correction, an air cavity effect and a wall effect. The air cavity effect is caused by 'in-scattering' that arises from inadequate guarding of the chamber or too small a diameter to height ratio. The wall effect is due to the non-water equivalence of materials from which the chamber is constructed.

The very small width of the guard ring of the Classic Markus chamber leads to a pronounced in-scattering cavity effect caused by electrons entering the cavity from the sides of the chamber as well as through the front face. This effect causes significant perturbation and so these chambers require a large perturbation correction to be applied. A further correction is required due to particles scattered back into the volume from the several millimetres of Perspex situated behind the collecting volume. McEwen *et al* (2001) demonstrated that the perturbation correction for the Classic Markus chamber might not have been accurately determined as was previously assumed. Significant chamber-to-chamber differences in the perturbation correction were found which might account for the differing values reported for the Markus perturbation correction by various authors.

McEwen *et al* (2001) measured large variations in the polarity correction between different chambers for the Classic Markus style of ionisation chamber. For this design of chamber differences in the polarity correction of up to 1% were seen with significant chamber-to-chamber variations due to the manufacturing process. It was also shown that recombination corrections for Classic Markus chambers were quite variable. These factors demonstrated that this design of chamber was not suitable for reference dosimetry.

However, the Markus style of chamber does have some advantages for certain applications. It was the first chamber to be designed specifically for electron dosimetry and has a small measuring volume of 0.055 cm^3 compared to the measuring volumes of the NACP-02 chamber (0.16 cm^3) and PTW Roos chamber (0.35 cm^3). The very small measuring volume of the Classic Markus chamber means that it has excellent spatial resolution and can be useful for small-field work or regions of high dose gradient with electron beams.

Two types of ionisation chamber have been designed to take account of the problems of the Classic Markus chamber, the Exradin A10 and the Advanced Markus. The construction details of both are given in table 2, taken from the manufacturers' data.

Chamber	Materials	Window thickness	Electrode spacing (mm)	Collecting electrode diameter (mm)	Guard ring width (mm)
Advanced Markus, type 34045	Polyethylene foil window Acrylic (PMMA) electrode PMMA cap	0.9 mm (incl. cap)	1	5.0	2
Exradin A10	Conductive kapton film front window Collector and guard – Shonka air-equivalent plastic Acrylic cap	Cap 1.0 mm	2	5.4	4

Table 2. Characteristics of Advanced Markus and Exradin A10 chambers

An Exradin A10 chamber has a collecting volume of 0.051 cm^3 and the same plate separation and dimensions as the Classic Markus chamber. The guard ring of an Exradin A10 chamber is 4 mm wide, much larger than that of the Classic Markus chamber. McEwen (2001) carried out some tests on one Exradin A10 chamber. A summary of the results of these tests can be seen in tables B1 and B2 of the Appendix. These results demonstrated that this particular Exradin A10 chamber showed a much larger polarity correction than a particular Markus chamber tested at the same time, and the magnitude of the correction was of the order of 1.5% at a nominal energy of 4 MeV. The polarity correction for the NACP-02 type chamber is less than 0.2% at all energies. There was nothing apparent in the design of the Exradin A10 to suggest why it should exhibit such a large polarity effect. It also exhibited a large value for the initial recombination and a non-zero perturbation correction. The work of McEwen (2001) only looked at one example of the Exradin A10 type ionisation chamber and so further work looking at several chambers was required to determine its suitability for use as a reference chamber.

The Advanced Markus ionisation chamber has also been designed to improve on the performance of the Classic Markus. It has a smaller measuring volume of 0.02 cm^3, and a much wider guard ring, of 2 mm, which was expected to reduce the perturbation effects exhibited by its predecessor. The wider guard ring was also expected to ensure that the effective point of measurement of the chamber was on the inside of the front entrance foil, rather than situated 0.5 mm behind it, as in the case of the Classic Markus chamber.

The manufacturers drawings for both the Advanced Markus ionisation chamber, type PTW 34045, and the Exradin A10 chamber are shown in figures 3 and 4 below. All dimensions are in millimetres.

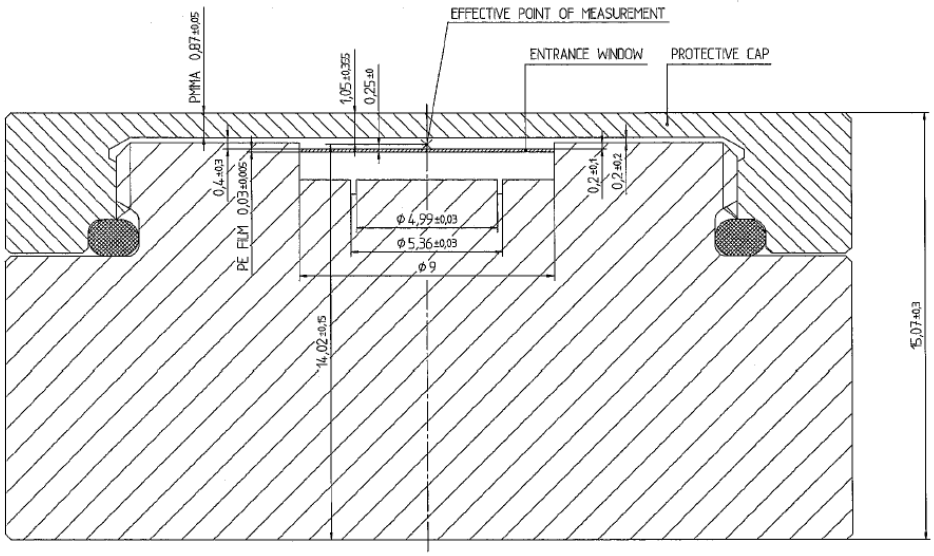

Figure 3. Manufacturer's drawing of the Advanced Markus ionisation chamber

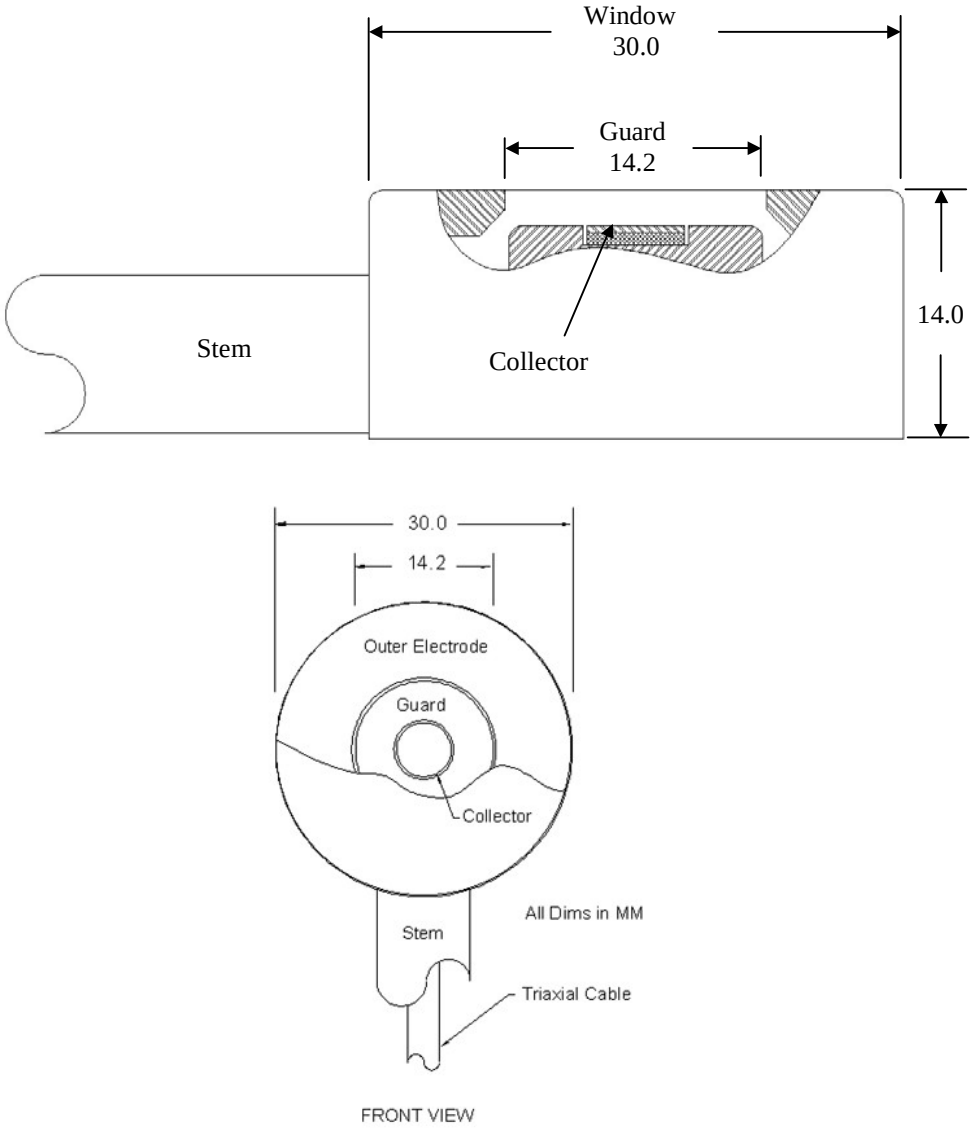

Figure 4. Manufacturer's drawings of the Exradin A10 ionisation chamber

3 THEORY

3.1 Determination of absorbed dose to water calibration factor

The reference depth of an ionisation chamber in water is determined from a depth-dose curve, as shown in figure 5.

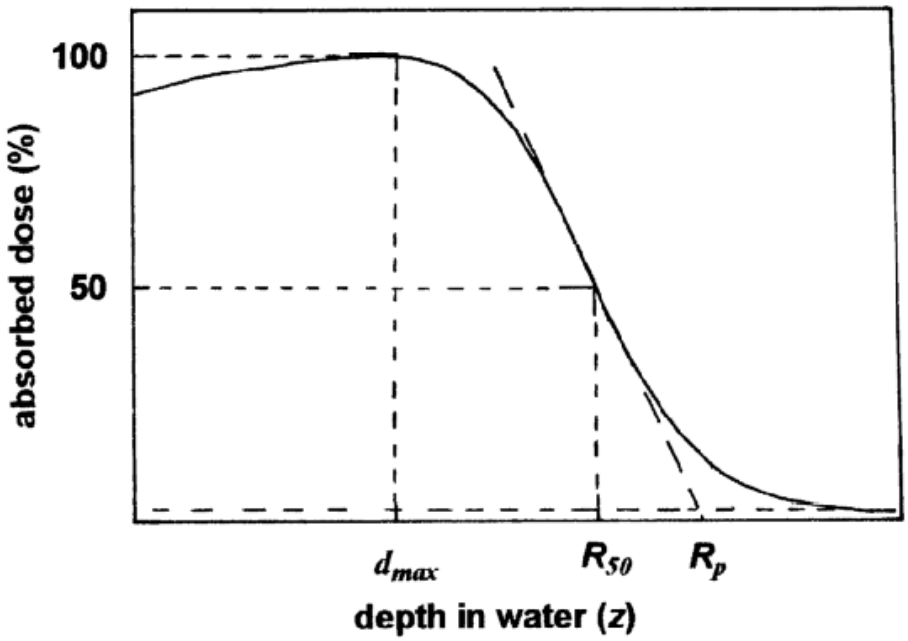

Figure 5. The depth-dose response of an ionisation chamber

It can be seen from the curve that the dose initially increases with depth, reaching a maximum of absorbed dose, D_{max} at depth d_{max}. R_{50} is the depth at which the dose is 50% of D_{max}, as shown.

The reference depth of an ionisation chamber in water, $d_{ref,}$ is given by Burns *et al* (1996) as

$$d_{ref} = 0.6R_{50} - 0.1\,\text{cm} \qquad (1)$$

3.1.1 Graphite calibration factors

The NPL has three reference chambers, all Scanditronix NACP-02, that are compared with the primary standard electron-beam graphite calorimeter. McEwen *et al* (1998a) describe the method of calibrating the reference chambers against the graphite calorimeter in more detail.

The NPL primary standard electron-beam graphite calorimeter consists of a graphite core and a graphite jacket. The graphite core is a disc of thickness 2 mm and diameter 50 mm. Two calibrated thermistors are embedded in the core. These enable the temperature rise within the graphite produced by an incident radiation beam to be accurately measured. The core is thermally isolated from the graphite jacket by a 1 mm air gap. The reference depth in graphite is chosen so that the electron spectrum at this depth in graphite is very similar to the equivalent scaled depth in water.

The reference depth in graphite, d_g, is given by

$$d_g = \frac{R_{50,g}}{R_{50,w}} d_{ref} \tag{2}$$

where $R_{50,g}/R_{50,w}$ is the ratio of the depths at which the dose is 50% of the maximum dose for graphite and water, and d_{ref} is the reference depth in water, as given in equation (1).

The absorbed dose, D_g, to the graphite core is determined directly

$$D_g = c_g T \tag{3}$$

where c_g is the specific heat capacity of the core, and T is the absolute temperature rise that is measured.

Reference chamber measurements are made in a graphite phantom under the same irradiation conditions as used for the calorimetry. The reference point of the reference chamber is positioned at the same depth in graphite as the centre of the calorimeter core.

The absorbed dose to graphite calibration factor, $N_{ref,g}$, is then determined using equation (4)

$$N_{ref,g} = \frac{D_g}{M_{ref,g}} \tag{4}$$

where D_g is the dose measured by the calorimeter, as given by equation (2), and $M_{ref,g}$ is the chamber reading at depth d_g in graphite, corrected for temperature, pressure, ion recombination and polarity.

The NPL reference ionisation chambers are calibrated in absorbed dose to graphite by substitution at seven electron energies. The graphite calibration factors for the NPL reference chambers are shown in table C1 of the Appendix.

3.1.2 Conversion from graphite to water

The absorbed dose calibration factors for the reference chambers must be converted from graphite to water using the theoretical conversion shown in equation (5).

$$N_{ref,w} = N_{ref,g} \frac{p_{ref,w}}{p_{ref,g}} \frac{s_{w/air}}{s_{g/air}} \quad (5)$$

where $N_{ref,w}$ is the absorbed dose to water calibration factor; $p_{ref,w}$ / $p_{ref,g}$ is the ratio of perturbation corrections in water and graphite for NPL reference chambers, and $s_{w/air}$ / $s_{g/air}$ is the effective stopping power ratio, water to graphite, taking into account the air volume of the chamber.

3.1.2.1 Stopping power ratio

The effective stopping power ratio, $s_{w/air}$ / $s_{g/air}$, is described by McEwen *et al* (1998b). The method used to determine the stopping powers combined Monte Carlo simulations of the experiment with measured electron depth-dose curves. The stopping power ratio at the reference depth used for each energy is given in table D1 in the Appendix.

3.1.2.2 Perturbation correction

The guarding of the NACP-02 ionisation chamber is such that it is assumed this type of chamber has a zero perturbation. This assumption was confirmed by Williams *et al* (1998) when Monte Carlo techniques were used to calculate the water to graphite perturbation factor ratios. Their results showed that the values of the water to graphite cavity perturbation factor ratio were approximately unity. They were unable to make accurate measurements of the wall perturbation ratio and so an assumed value of 1.000 is assigned for the perturbation correction.

3.1.3 Calibration of users ionisation chamber

The users ionisation chamber is calibrated in terms of absorbed dose to water using the method of direct replacement in a water phantom against the NPL reference chambers at seven electron energies.

The absorbed dose to water calibration factor for a user chamber, $N_{user,w}$, is given by

$$N_{user,w} = N_{ref,w} \frac{M_{ref,w}}{M_{user,w}} \quad (6)$$

where $N_{ref,w}$ is the mean water calibration factor for the set of NPL reference chambers from equation (5), and $M_{ref,w}$ / $M_{user,w}$ is the ratio of reference and user chamber measurements in water.

3.1.4 Polarity correction

A correction for polarity effects must be applied to all chamber readings at each of the seven energies used. The polarity correction is given in the IPEM Code of Practice (IPEM 2003) as

$$f_{pol} = \frac{\left|M^{+}\right| + \left|M^{-}\right|}{2M} \tag{7}$$

where the superscripts "+" and "–" indicate the polarity of the polarising voltage for chamber reading M, and the M in the denominator is the reading taken with the normal polarity used during measurements.

3.1.5 Ion recombination correction

General recombination in an ionisation chamber is dependent on the polarising voltage applied and on the dose-per-pulse.

A plot of the reciprocal of the ionisation current against the reciprocal of the polarising voltage should be a straight line over the voltage range used in these measurements, according to Boag theory (Boag and Currant (1980)). The recombination correction is then calculated from these measurements for a particular polarising potential at any dose-rate, as given by Burns and McEwen (1997).

$$f_{ion} = c + md \tag{8}$$

The parameters c and m are the y-axis intercept and gradient of the plot. The parameter d is the dose-per-pulse.

4 METHOD

4.1 Ratio of reference and user chamber measurements

The ionisation chambers under investigation were calibrated directly against the three NPL reference ionisation chambers in a water phantom. The water phantom was filled with demineralised water and positioned on the experimental table in the exposure room at a source-to-surface distance of 2.0 m. All equipment was left in the exposure room over night to equilibrate to room temperature. The water phantom has been specifically designed to enable different chamber types to be positioned with their measurement reference point at the correct reference depth in water, d_{ref}, for each nominal beam energy. Seven nominal beam energies are used at the NPL: 4, 6, 8, 10, 12, 16 and 19 MeV, each having a particular reference depth dependent on factors in equation (1) obtained from their depth dose curves (figure 5). The field was circular and 15 cm in diameter at the phantom surface.

Each Advanced Markus chamber was supplied with a waterproof cap that screwed onto the chamber before immersion in water. The Exradin A10 was supplied with a waterproof cap that relied on a simple pressure fit to keep it in place.
A transmission monitor chamber was mounted approximately 15 cm in front of the water phantom. A 1 cm thick lead collimator with a 15 cm diameter hole was centred on the transmission monitor. The transmission monitor was used as the transfer instrument between the chambers under investigation and the NPL reference chambers. Calibrated thermistors were attached to both the water phantom and transmission monitor to enable a temperature correction to be applied to each measurement, and a calibrated barometer was used to determine the pressure correction. All readings were corrected to the standard conditions of 20°C (293.15 K) and 101.325 kPa.

A polarising voltage of –100 V was applied to both the NPL reference chambers and the chambers under investigation. The linear accelerator was set to operate at a dose-rate of approximately 2 Gy/min at the point of measurement. This is a similar dose-rate to that used for patient treatment in the clinic. The transmission monitor chamber and ionisation chamber were connected to Keithley 617 electrometers in external feedback mode using a calibrated capacitor in each feedback circuit. A computer running software written at NPL was used to control the in-beam readings where the charge accumulated in approximately 20 s from each chamber was measured. The computer-controlled system also recorded the temperature and pressure and their associated corrections with each reading taken.

Figure 6 shows the experimental set-up that was used for the measurements in the exposure room at the NPL.

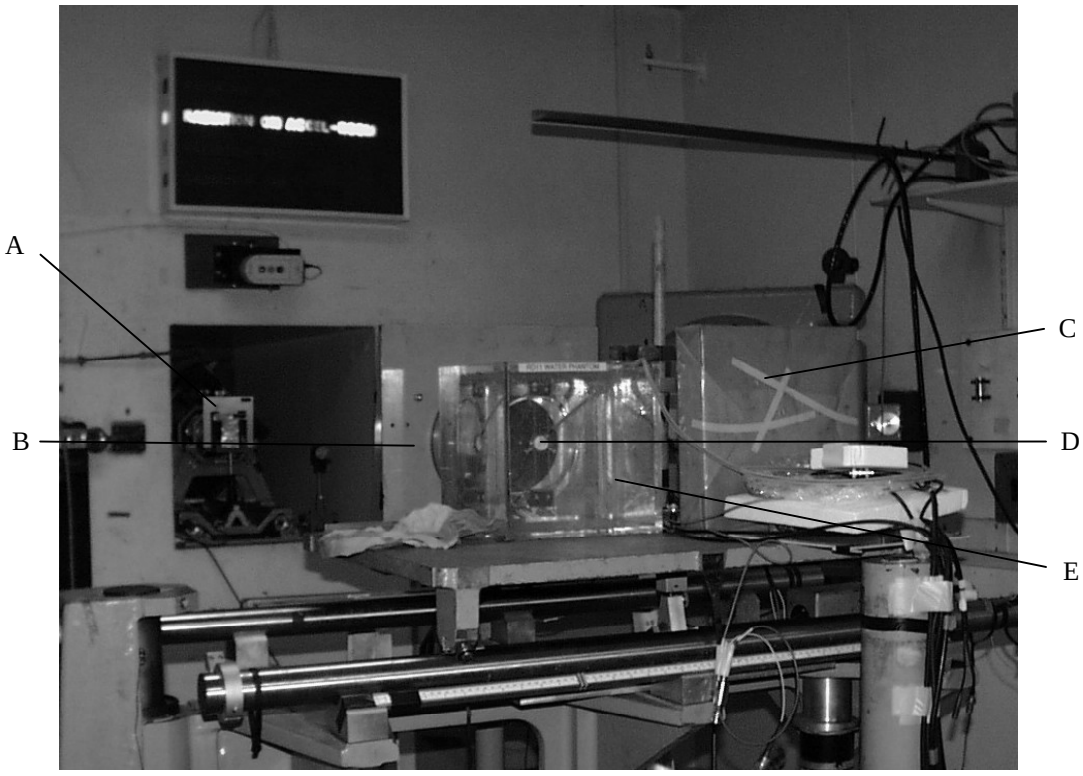

Figure 6. The experimental set-up for ionisation chamber calibrations at the NPL

A focused beam of electrons are accelerated down through the flight tube and scattered as they hit the aluminium scatter plates placed at (A). Different thicknesses of scatter plate are used for each nominal beam energy. (B) is the transmission monitor in a steel surround, on to the front of which the lead collimator is placed (not visible here). A calibrated thermistor is attached to the transmission monitor. (C) is a graphite block used to shield the cables connected to the thermistors, ionisation chamber and transmission monitor. This is to minimise the amount of radiation dose the cables will receive. (D) is the ionisation chamber positioned at the reference depth in the water phantom (E) on the experimental table. There is a calibrated thermistor connected to the water phantom to record the temperature of the ionisation chamber. To provide some scale it may be noted that the water phantom is a 26 cm cube.

The order of measurements was as follows:

1. NPL reference chambers
2. Chambers under investigation
3. NPL reference chambers (to measure linac or measuring system drift).

Before each set of measurements a radiation-induced leakage current test was performed on each ionisation chamber, including the NPL reference chambers. This test involved exposing each chamber to a beam of electrons from the linear accelerator for approximately 20s. After this time the electrometers measured a voltage developed across the feedback capacitor as a result of the charge collected from the ionisation current from the chamber. A significant variation in recorded voltage as a function of time elapsed since the beam was turned off indicated a fault in the chamber. None of the chambers used in this study indicated a radiation-induced leak at any time.

4.2 Polarity measurements

The polarity correction was calculated for each chamber at each nominal beam energy, by taking a series of chamber readings with an applied voltage of –100 V and then, under the same irradiation conditions, taking further readings at +100 V. To correct for any drift due to the linear accelerator or measurement system, the initial reading with the chamber operating at –100 V was repeated. The symbol $|\bar{M}|$ in equation (7) represents the average of the two readings taken with the chamber operating at –100 V.

In this case the normal polarity used during measurements was –100 V, so the symbol M in the denominator of equation (7) is also the average of the two readings taken with negative polarity.

4.3 Ion recombination measurements

General ion recombination is dependent on the polarising voltage applied and the dose-per-pulse, so recombination measurements were made with each chamber at four different dose-rates between 1 and 8 Gy/min and at a pulse frequency of 240 Hz. The polarising voltage on each chamber was varied in steps between the calibration voltage (–100 V) and a value of –30 V.

4.4 Radiographs

The diagnostic X-ray set at the NPL was used to take radiographs of all four chambers. These allow a check that both the internal and external construction of a chamber are consistent with the manufacturers' drawings, and may also show up any damage. A radiograph of each chamber was taken both face on and from the side. The diagnostic X-ray set was operated at 40 kVp with a current of 100 mA and 3.2 mAs.

4.5 Check source measurements

Check source measurements were carried out on each chamber several times both before and after the calibrations using the NPL check source system. Ionisation chambers are fragile and can have faults with very little or no visible sign of damage. In view of the fact that they are so delicate, a radioactive source can be used to check the overall sensitivity of the chamber and a corresponding measuring assembly. It is possible to use the chamber in the usual way to determine the ionisation current. The decay constant of the source is well known and so the ionisation current on any date can be corrected back to the previous measurement. Any disagreement greater than the random variation would indicate that there might be a fault with the chamber.

The NPL check source system comprises a strontium-90 check source, a calibrated electrometer, a calibrated thermometer and a calibrated barometer. The check source is a strontium-90 radioactive source that was placed on a modified NPL source holder over the front face of the chamber. The chamber was connected to the electrometer and a voltage of –100 V was applied. Charge was collected for a fixed period of time. Five measurements of charge collected in a fixed time were taken for each chamber and the mean determined. Measurements of temperature and pressure were made and the mean charge corrected for temperature and pressure to the standard conditions of 293.15 K and 101.325 kPa. The mean charge was converted to current and then corrected for radioactive decay to a particular reference date. The readings of current measured on each occasion could then be compared for the duration of the project.

Strontium-90 check source measurements are regularly used at the NPL to monitor ion chamber stability. The natural leak of each chamber was also measured during these measurements by looking at the charge recorded on the electrometer without the strontium-90 check source in position. None of the chambers under investigation exhibited a natural leak at any time during the measurements.

Measurements of current from the chambers when exposed to the strontium-90 check sources were also carried out on each chamber. This can be used to show a chamber settling. A voltage of –100 V was applied to the ionisation chamber and it was left to settle for 30 minutes. After this time the strontium-90 check source was placed on the check source holder over the chamber. A computer controlled acquisition system was then used to measure the chamber ionisation current using a Keithley 6517 electrometer, and the corresponding temperature and pressure were also recorded at intervals of approximately 2 s. The variation in the ionisation current as a function of time was used to demonstrate the settling characteristics of the chamber.

4.6 Response in a clinical beam

On completion of the calibration the chambers were taken to Norfolk and Norwich Hospital for testing. Norfolk and Norwich Hospital has a Varian linear accelerator that can operate at nominal energies of 6, 9, 12, 16 and 20 MeV. The beam quality specifier is the quantity $R_{50,D}$. It was decided to test the chambers at two energies on the clinical accelerator that had values of $R_{50,D}$ and hence $d_{ref,w}$ near to those of the NPL linear accelerator. The 10 MeV nominal energy at the NPL has $d_{ref,w}$ of 1.99 cm while the Norfolk and Norwich clinical 9 MeV has $d_{ref,w}$ of 2.04 cm. The 19 MeV nominal energy at the NPL has $d_{ref,w}$ of 3.86 cm while the Norfolk and Norwich clinical 16 MeV has $d_{ref,w}$ of 3.93 cm.

Previous work on the Classic Markus chamber by McEwen *et al* (2001) showed that the calibration factor and polarity correction were sensitive to the different electron beams of a hospital linear accelerator and the NPL linear accelerator. Therefore measurements taken on a clinical linear accelerator at a hospital may show if this were also the case for the Advanced Markus and Exradin A10 chamber types. A NACP-02 type chamber and a Roos type chamber were also taken to test, as these chambers should show no variation in different accelerator beams.

The measurements that were made in the clinical beam were a subset of those that were made at the NPL. The water phantom was positioned on the treatment couch in front of the accelerator head (figure 7) at a source-to-surface distance (SSD) of 100 cm with a 14 cm diameter field size at isocentre. The transmission monitor was mounted on the front of the water phantom. Thermistors were attached to both the water phantom and transmission monitor. A computer controlled data acquisition system was used to take the measurements in the same way as at the NPL.

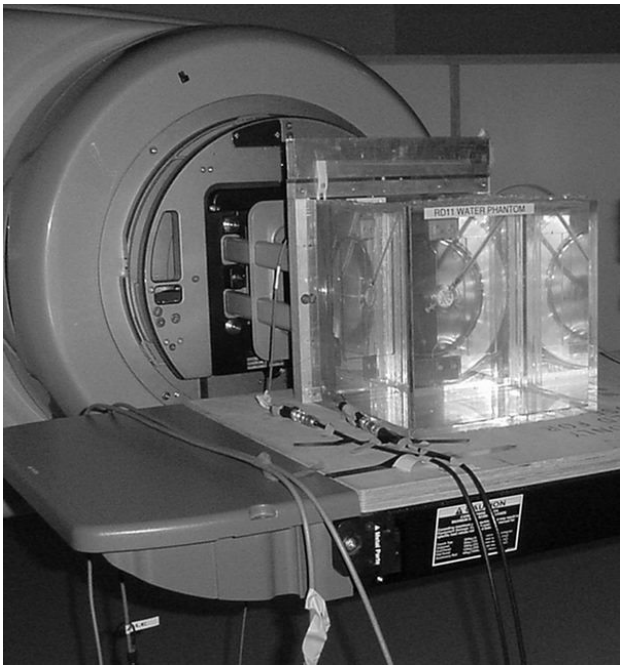

Figure 7. The apparatus set-up at Norfolk and Norwich Hospital

The three NPL reference chambers were put in the beam at the beginning and end of each day. The three Advanced Markus chambers and the Exradin A10 chamber were calibrated in the clinical beam at both 9 and 16 MeV. Polarity measurements were carried out at both energies. Recombination was investigated for each of the four chambers at just 9 MeV and only at one dose-per-pulse. The dose-per pulse could not be changed for the clinical accelerator.

4.7 Analysis of data

The chamber under test (the 'standard') and the transmission monitor chamber were connected to separate electrometers in charge integration mode using calibrated external feedback capacitors. While the chambers were being exposed, the standard and monitor electrometers were triggered simultaneously to integrate charge for 20 s. The ratio of the standard to monitor readings was then calculated. This process was repeated at least four times to ensure that the ratio was constant within normal experimental variation. The mean of the standard to monitor ratio for each set of measurements was corrected for temperature and pressure variations.

The polarity correction was determined from the data using equation (7). The recombination measurements were plotted and it was possible to determine the gradient and intercept of the line described by equation (8). The gradient and intercept of this line could then be used to determine the recombination correction, f_{ion}, for each chamber at each energy. This was achieved using equation (9) below.

$$f_{ion} = \frac{1000\ x\ cap}{prf\ x\ dt}.uncorr\ std/mon.\frac{mon\ V}{HT}.gradient + intercept \qquad (9)$$

where *cap* is the value of the feedback capacitor; *prf* is the pulse repetition frequency of the linear accelerator; *dt* is the integration time; *uncorr std/mon* is the ratio of the voltage recorded on the standard to that of the transmission monitor before any polarity or ecombination corrections have been applied; *mon V* is the value of the voltage recorded on the monitor only, and *HT* is the voltage that is applied to the ionisation chamber.

The corrected standard to monitor ratio was obtained by multiplying the uncorrected ratio by the calculated recombination and polarity corrections. No corrections for either depth or uniformity were required.

The transmission monitor was used as the transfer instrument between the three NPL reference chambers and the chambers under investigation. It was calibrated using the NPL reference chambers. The corrected standard to monitor ratio for the NPL reference chambers was multiplied by the correct absorbed dose to graphite calibration factor for the particular reference chamber, the stopping power ratio and the perturbation ratio. This was repeated for each reference chamber and over the course of the day a mean of all transmission monitor calibration factors was obtained. The calibration factor for each chamber under test was determined by dividing the mean transmission monitor calibration factor by the corrected standard to monitor ratio for the individual chamber. This is described by equation (6).

The results from Norfolk and Norwich Hospital were analysed using an identical method. However the prf of the Varian linear accelerator was approximately 30 Hz and the recombination was only determined at one particular dose-per-pulse. Equation (8) was used to determine the recombination correction for each chamber at each energy. The dose-per-pulse of the Varian linear accelerator was 0.11 cGy/pulse at 9 MeV and 0.101 cGy/pulse at an energy of 16 MeV.

5 RESULTS

5.1 Radiographs

Radiographs of one Advanced Markus type chamber and the Exradin A10 chamber are shown in figures 8 and 9 respectively. Parallel-plate ionisation chambers are constructed from low-Z plastics so it is often difficult with radiographs to obtain sufficient contrast between the various components that constitute the chamber.

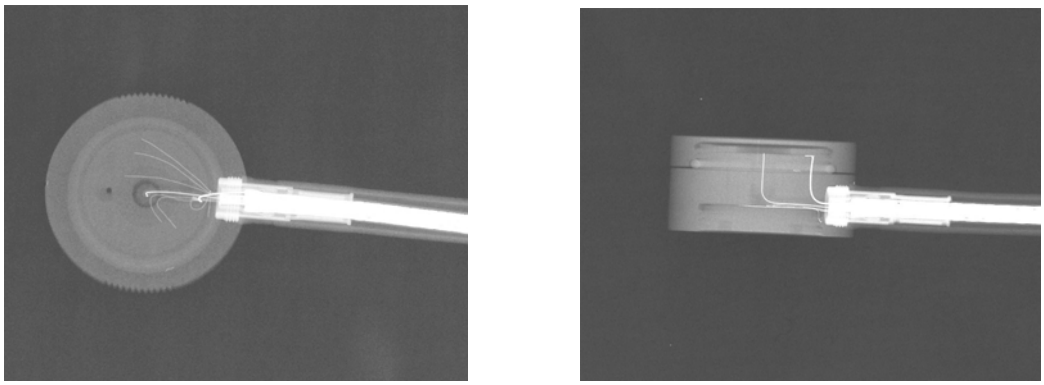

Figure 8. Radiographs of an Advanced Markus type ionisation chamber

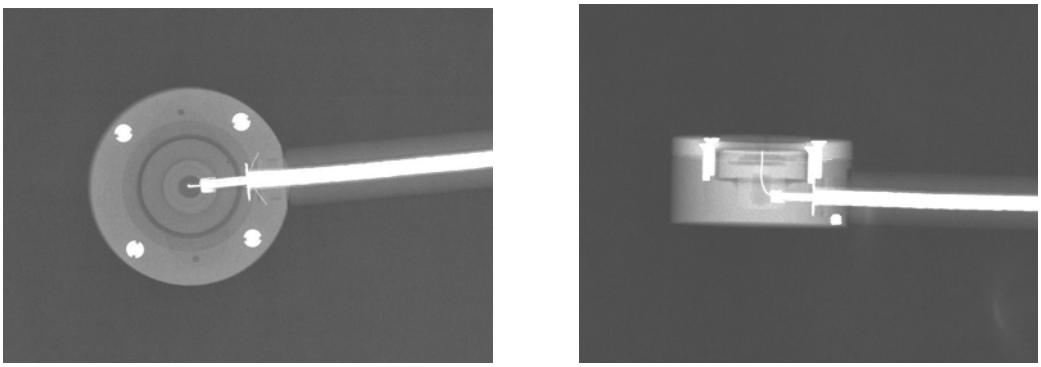

Figure 9. Radiographs of an Exradin A10 type ionisation chamber

5.2 Check source measurements

Check source measurements were carried out on each chamber over a period of 130 days. Figure 10 shows the relative response of each chamber normalised to the respective mean as a function of days elapsed since the first measurement. The standard uncertainty associated

with each measurement is ± 0.2%; this is illustrated on the results for Advanced Markus chamber 0088.

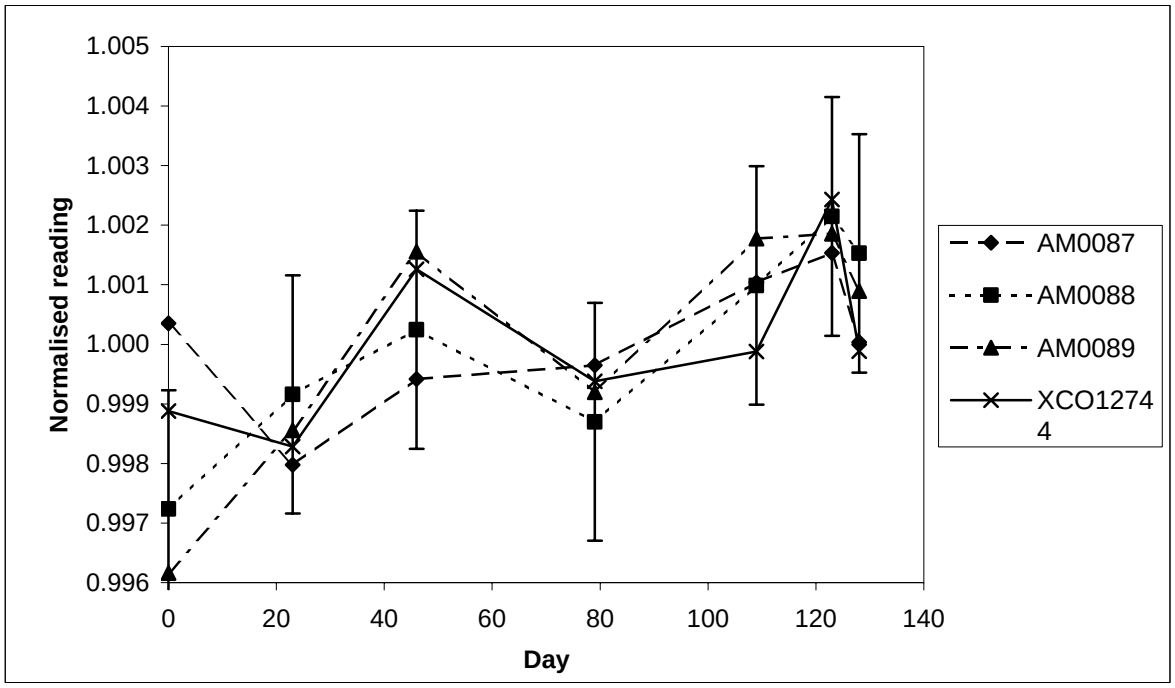

Figure 10. Strontium-90 check source measurements corrected for source decay

Figures 11 and 12 show typical results of the continuous current measurements made using a strontium-90 radioactive source. The graphs are normalised to the average of the final 100 readings of current that were recorded for each chamber.

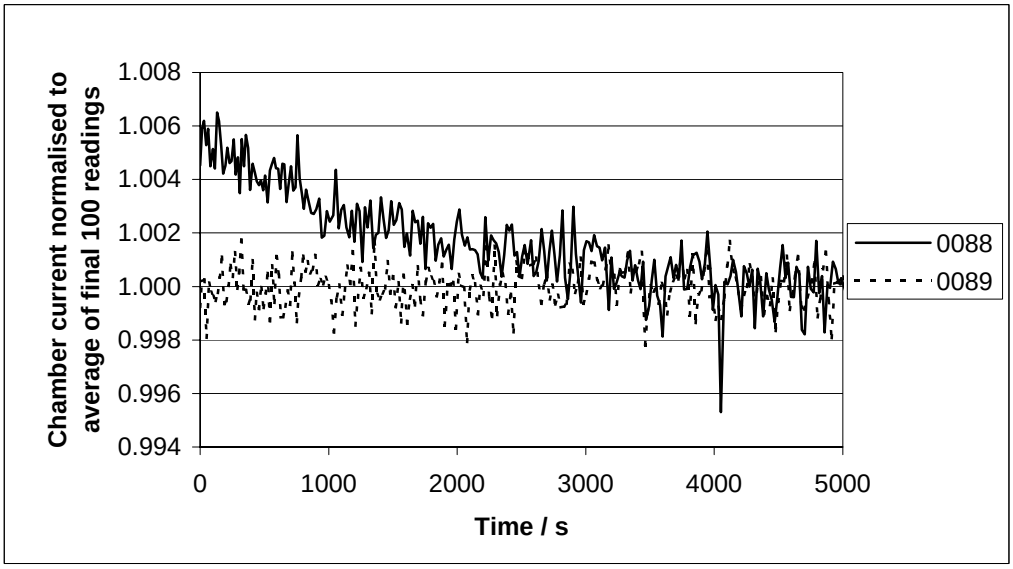

Figure 11. Continuous current measurements for Advanced Markus type

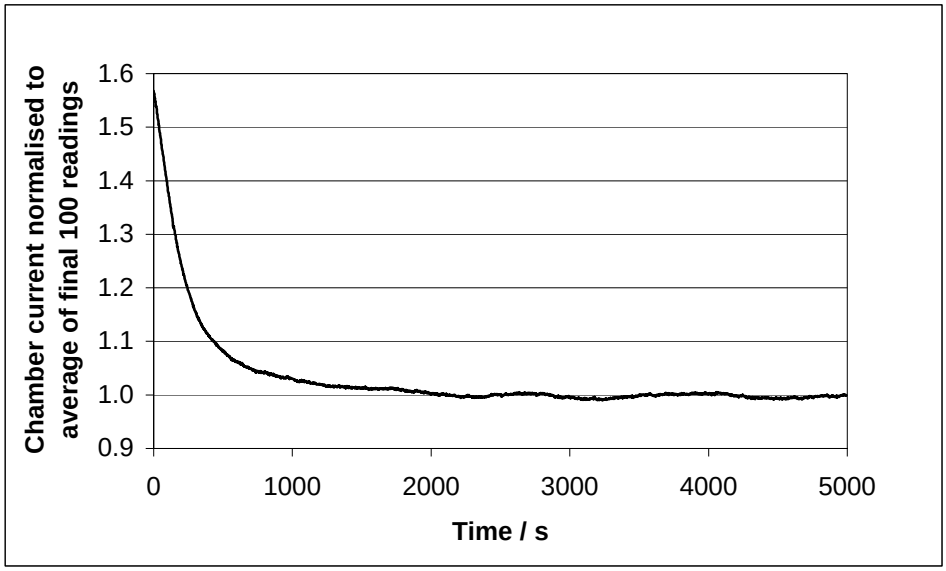

Figure 12. A continuous current measurement for Exradin A10 chamber

5.3 Absorbed dose to water calibration factor

The absorbed dose to water calibration factors that were determined for each chamber are shown in table 3. A graph showing the variation in calibration factor as a function of the beam quality specifier $R_{50,D}$ is shown in figure 13. The scale on the left refers to the Advanced Markus chambers; that on the right is for the Exradin A10 chamber. Scales left and right represent an increase in calibration factor of 1.1%. The standard uncertainty associated with each calibration factor is ± 0.75%. The components that make up this uncertainty are given in table E1 of the Appendix.

E_{nom} (MeV)	$R_{50,D}$ (cm)	$N_{u,w}$ (Gy/μC) AM0087	$N_{u,w}$ (Gy/μC) AM0088	$N_{u,w}$ (Gy/μC) AM0089	$N_{u,w}$ (Gy/μC) XCO12744
4	**1.23**	1319.87	1316.03	1304.66	543.22
6	**1.97**	1315.18	1307.06	1292.95	549.63
8	**2.75**	1300.50	1293.22	1278.34	548.36
10	**3.48**	1282.80	1278.66	1262.55	547.84
12	**4.23**	1277.32	1270.72	1258.83	543.95
16	**5.72**	1261.32	1256.48	1242.69	536.20
19	**6.60**	1250.57	1244.62	1230.17	531.27

Table 3. Absorbed dose to water calibration factors

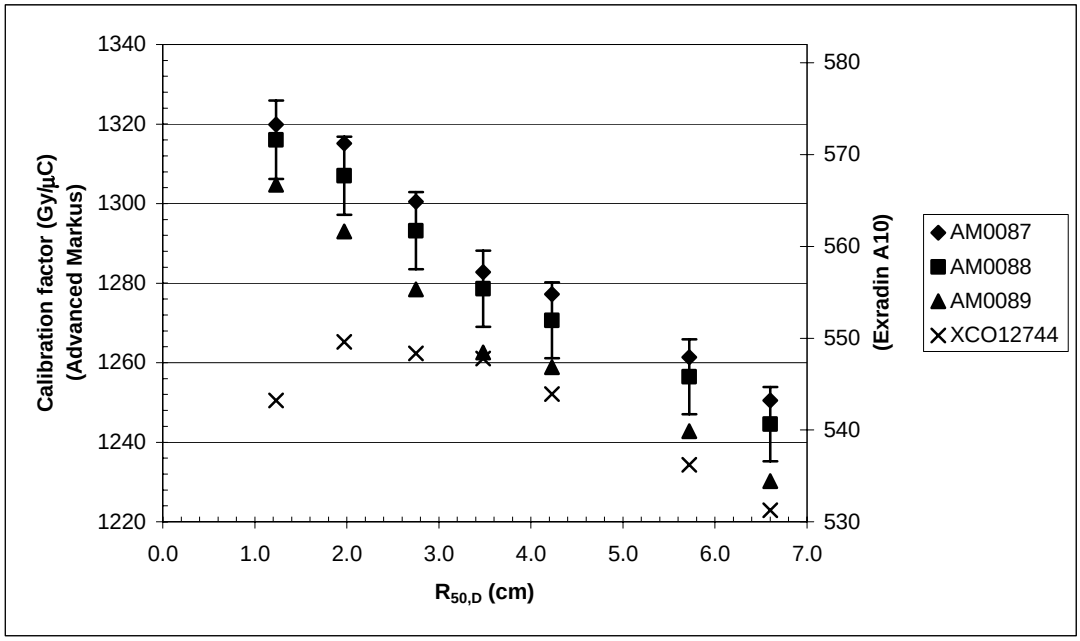

Figure 13. Absorbed dose calibration factors as a function of $R_{50,D}$

5.3.1 Polarity correction

Measurements of the polarity correction were made for each chamber at all energies. The results are given in table 4 and shown as a function of $R_{50,D}$ in figure 14. The standard uncertainty associated with each measurement of the polarity correction is ± 0.1%.

E_{nom} (MeV)	**$R_{50,D}$ (cm)**	**Correction to negative polarity AM0087**	**Correction to negative polarity AM0088**	**Correction to negative polarity AM0089**	**Correction to negative polarity XCO12744**
4	**1.23**	0.9740	0.9753	0.9718	0.9810
6	**1.97**	0.9865	0.9863	0.9831	0.9874
8	**2.75**	0.9915	0.9914	0.9875	0.9904
10	**3.48**	0.9950	0.9945	0.9913	0.9910
12	**4.23**	0.9987	0.9989	0.9955	0.9938
16	**5.72**	0.9979	0.9993	0.9960	0.9945
19	**6.60**	0.9978	1.0002	0.9967	0.9958

Table 4. Polarity corrections for all chambers

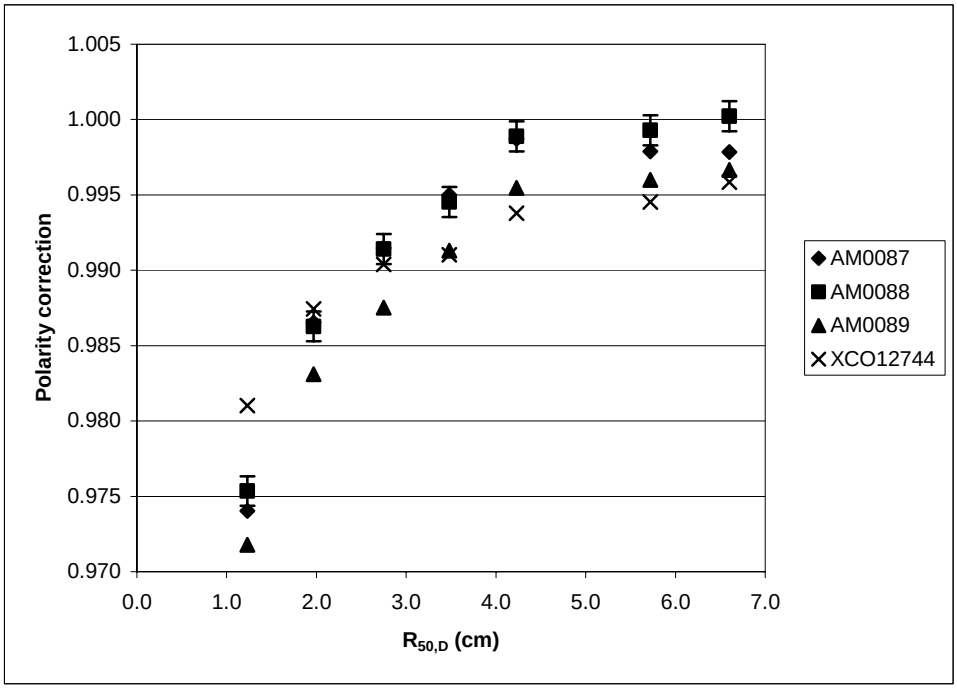

Figure 14. Polarity correction as a function of $R_{50,D}$

5.3.2 Ion recombination correction

A typical plot of the reciprocal of the ratio of the voltage recorded on the chamber to that of the transmission monitor as a function of the reciprocal of the polarising voltage is shown in figure 15. This particular recombination measurement is for Advanced Markus ionisation chamber 0089 at a dose-per-pulse of 0.035 cGy and a dose-rate of 5 Gy/min.

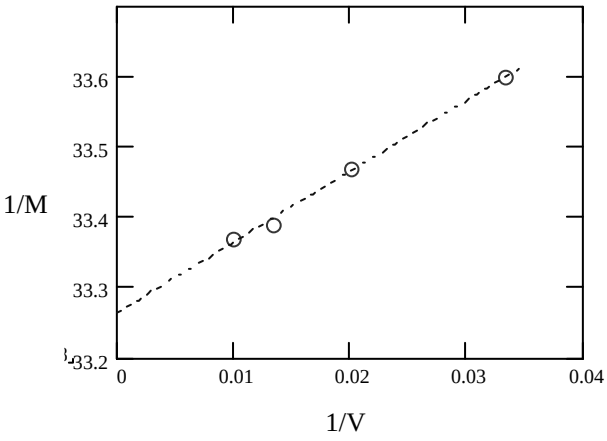

Figure 15. Ion recombination measurements

For each chamber, at four dose-rates, the gradient and intercept of the corresponding plot was calculated and the recombination correction for a particular dose-rate determined. Combining the data for all four dose-rates enabled the recombination coefficients to be determined.

The recombination coefficients in terms of the dose-per-pulse (as used in equation (8)) determined for Advanced Markus chambers 0087, 0088, 0089 and Exradin A10 chamber XCO12744 are given in table 5.

Chamber	*c*	*m*
AM0087	1.0022	0.0421
AM0088	1.0026	0.0308
AM0089	1.0012	0.0499
XCO12744	1.0057	0.2548

Table 5. Recombination coefficients

5.3.3 Perturbation correction

The ratio of each calibration factor to the combined response of several NACP-02 and Roos chambers was determined at each energy. This was normalised to the mean and the mean energy response as a function of $R_{50,D}$ is shown in figure 16. The 4 MeV point for Exradin A10 chamber XCO12744 has not been included in the analysis as it was considered anomalous. The relative energy responses of an NACP-02 chamber and Roos chamber calibrated at the same time are also shown in figure 16.

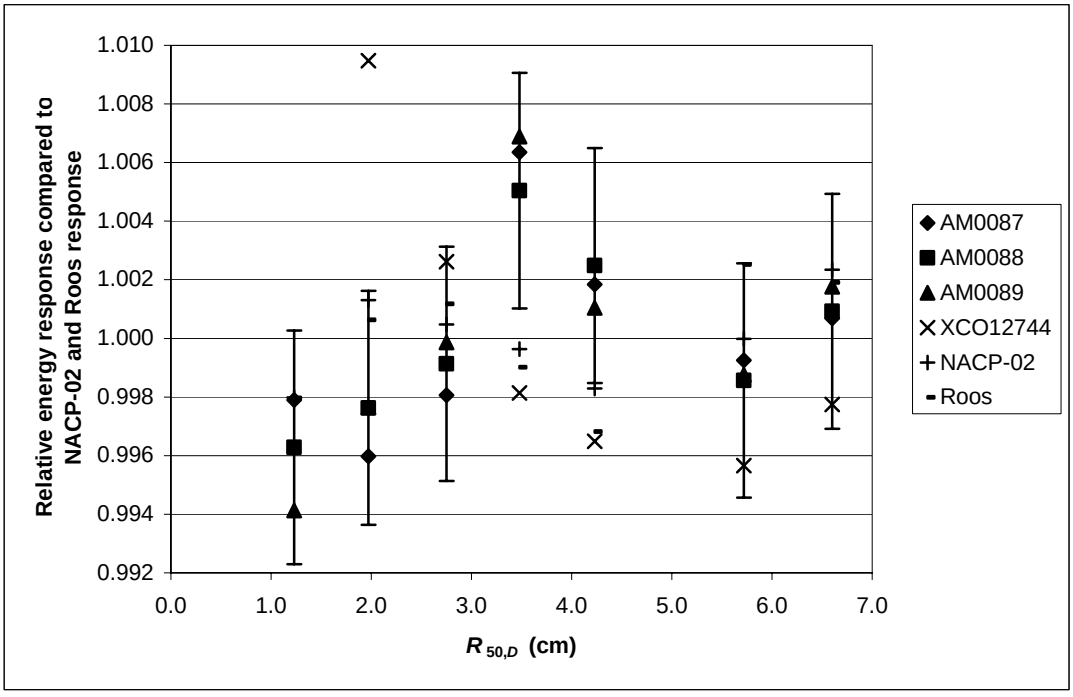

Figure 16. Relative energy response as a function of $R_{50,D}$

5.4 Clinical results

The measurements taken in the clinical beam at Norfolk and Norwich Hospital are displayed in figure 17 with the calibration data measured at the NPL. A straight line has been applied to the calibration data obtained from the measurements made at the NPL for each chamber. The equation of each line has been used to determine what the absorbed dose to water calibration factor should be at the appropriate $R_{50,D}$ in the clinical beam. All measurements have been corrected for pressure and temperature. Polarity and ion recombination corrections have also been applied. The standard uncertainty associated with each calibration factor is $\pm$ 0.75%, as in the case for the NPL measurements.

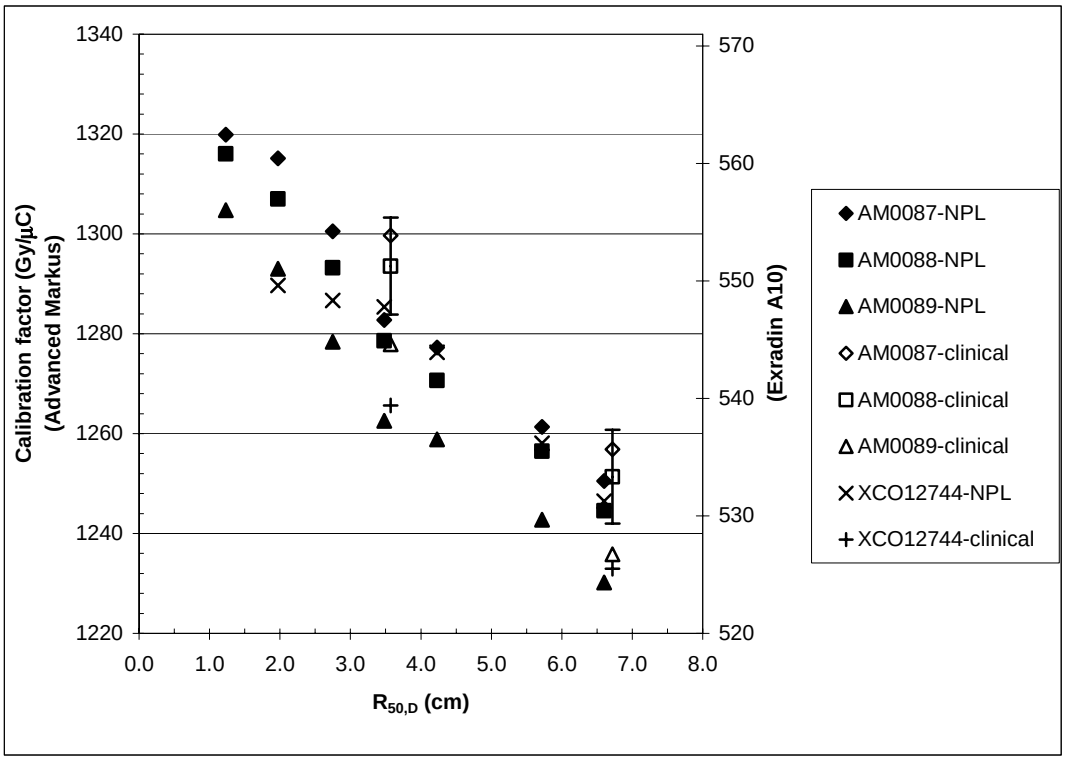

Figure 17. Calibration factors as a function of $R_{50,D}$ obtained in clinical beam

Table 6 shows the absorbed dose to water calibration factors predicted using the linear fits to the calibration factor obtained at the NPL. Also shown is the calibration factor as measured in the clinical beam and the spread between this and the predicted value.

Chamber		$N_{u,w}$ (Gy/mC) 9 MeV	$N_{u,w}$ (Gy/mC) 16 MeV
AM0087	**Clinical**	1299.67	1256.85
	NPL predicted	1288.63	1246.57
	Spread	*0.86%*	*0.82%*
AM0088	**Clinical**	1293.54	1251.35
	NPL predicted	1282.83	1246.57
	Spread	*0.83%*	*0.38%*
AM0089	**Clinical**	1277.87	1235.82
	NPL predicted	1269.18	1226.64
	Spread	*0.68%*	*0.75%*
XCO12744	**Clinical**	539.40	525.49
	NPL	545.14	532.13
	Spread	*-1.05%*	*-1.25%*
0227 (Roos)	**Clinical**	78.93	75.24
	NPL predicted	77.48	75.02
	Spread	*1.87%*	*0.29%*
DFA0006306 (NACP-02)	**Clinical**	143.52	139.42
	NPL predicted	143.68	139.04
	Spread	*-0.11%*	*0.27%*

Table 6. Absorbed dose to water calibration factors determined in the clinic

The polarity correction for each chamber was also determined in the clinical beam. These results are displayed graphically in figure 18. The measured polarity correction obtained in the NPL beams is also shown.

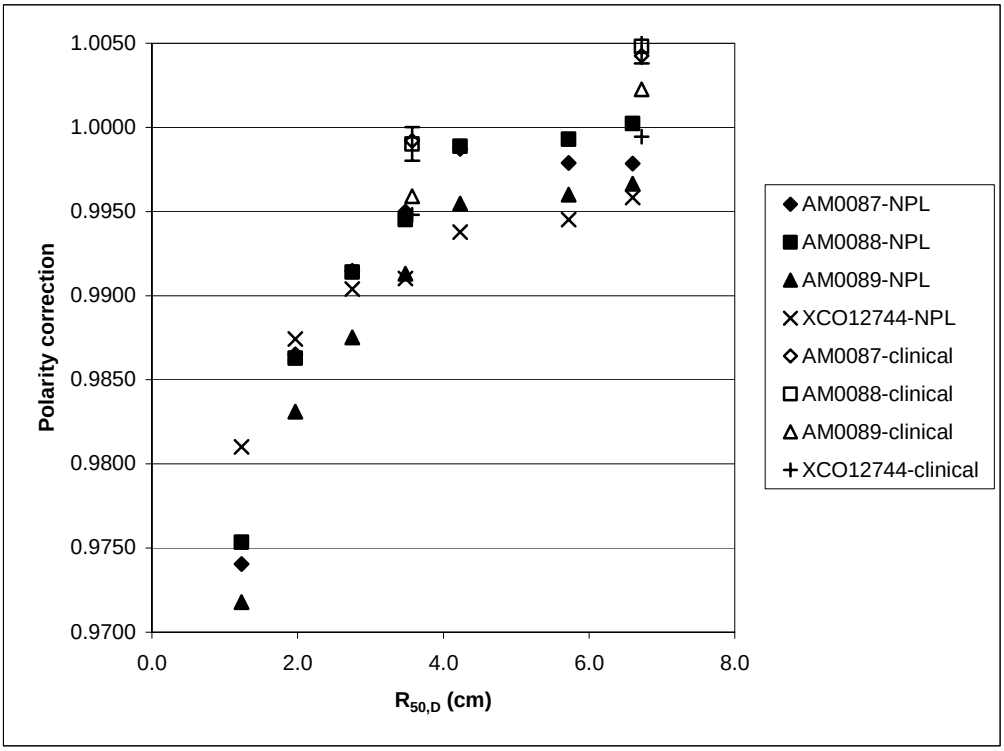

Figure 18. Polarity corrections in different beams as a function of $R_{50,D}$

6 DISCUSSION

6.1 Radiographs

From figure 8, the face-on radiograph of the Advanced Markus ionisation chamber, it is possible to see the components that make up the chamber. The HT electrode and collector wire can both be seen coming from the chamber stem. It can also be seen from the face-on radiograph that there are a series of earthing wires throughout the ionisation chamber body.

The side-on radiograph of this chamber shows more clearly the different parts that constitute the chamber and can be compared with the manufacturer's drawing in figure 3. This radiograph was taken with the waterproof cap on the chamber to make positioning it easier. The sensitive volume of the chamber is shown and appears as a small shadow just behind the waterproof cap. It is possible to see the HT electrode and collector wire applied to the plates. The earthing wires are not near the sensitive volume, the radiograph from this angle demonstrates clearly that they are situated in the plastic at the back of the chamber.

The face-on radiograph of the Exradin A10 ionisation chamber also demonstrates the components of the chamber. Two earthing wires can be seen at the bottom of the chamber and the collector wire is shown travelling from the chamber stem to the sensitive volume. The sensitive volume can be seen as a small dark circle at the centre of the chamber. There are four screws in this chamber holding the body together. These are made up of a high-Z material so their contrast is very good.

The side-on radiograph of the Exradin A10 was taken without the waterproof cap on. The collector can be seen passing to the rear of the sensitive volume. It is not possible in these radiographs to identify the HT electrode.

A comparison of all radiographs taken of each of the four chambers with the appropriate manufacturers' drawing indicated that there were no visible internal faults. A visual inspection of the outside of each chamber on arrival indicated that there were no external faults.

6.2 Check source measurements

The results of the check source measurements are shown graphically in figure 10. Each reading has been corrected to the standard conditions of 293.15 K and 101.325 kPa. Correction for source decay has been applied to each measurement. It can be seen that there is an upward drift on the sets of data for each chamber. The error bars on each check source measurement are given as ±0.2%. The maximum spread for each of the ionisation chambers is ±0.3%, which is similar to that for other chamber types. This spread is most likely due to relative positioning of the strontium-90 source and the chamber. Care was taken to ensure that the strontium-90 source and source holder were in the same position over the chamber for each measurement but this may not have always been the case.

The continuous current results for the Advanced Markus ionisation chambers are shown in figure 11. It can be seen that chamber 0089 settles to within 0.1% of its final value almost immediately. Chamber 0087 takes 2500 seconds (approximately 42 minutes) to settle from a reading 0.5% higher than the mean, and chamber 0088 takes 3000 seconds (50 minutes) to settle from a value 0.6% higher. This is much longer than the time that the chambers are left to settle in the electron beam of the linear accelerator. However, the ionisation current from an Advanced Markus chamber was measured as approximately 8 pA, compared to 25 pA during linac beam measurements. This is three times greater than the ionisation current from the strontium-90 check source. If it can be assumed that the chamber settling is more strongly dependent on the dose received rather than the time the chamber is exposed to the radiation, then these results indicate that the chamber would settle in the electron beam of the linear accelerator in a maximum time of 15 minutes. The Advanced Markus chambers were always left to settle for at least this length of time in the linear accelerator beam before data for analysis was collected. However, it is not always possible to predict stabilisation times from one radiation source to another, particularly between continuous radiation, as in the case of strontium-90, and pulsed radiation, as in the case of the linear accelerator.

The continuous current results for the Exradin A10 chamber, serial number XCO12744 are displayed in figure 12. The initial reading of current is 60% higher than the final value. It takes approximately 2000 seconds (33 minutes) for this chamber to settle to its final value and is within 10% after 500 seconds (about 8 minutes). Such extreme settling could be due to the settling of the system used to measure the current and may not be a reflection on the chamber. In the same way as before, the mean ionisation current due to the strontium-90 check source of 13 pA can be compared with the ionisation current of 62 pA in the linear accelerator beam. This is five times greater and so using the same assumption as for the Advanced Markus chambers, if the settling depends on dose alone, then this chamber should

settle in the linear accelerator electron beam in a time of 7 minutes. The Exradin A10 chamber was always left to settle before calibration for at least this length of time.

6.3 Absorbed dose to water calibration factors

The absorbed dose to water calibration factors for each ionisation chamber are shown in table 3, and graphically in figure 13.

The absorbed dose to water calibration factors for the Advanced Markus ionisation chambers are all of the order of 1300 Gy/μC. The small variations in calibration factor between each chamber are due to the slight differences in the size of the sensitive volume. It can be seen that as the beam quality specifier $R_{50,D}$ increases the absorbed dose to water calibration factor decreases. This decrease appears approximately linear and is a similar characteristic to that of other types of parallel-plate chambers. The change of calibration factor with $R_{50,D}$ is similar for all of the Advanced Markus chambers due to them having the same geometry.

The Exradin A10 ionisation chamber XCO12744 has absorbed dose to water calibration factors of the order of 540 Gy/μC. It can be seen that the calibration factors decrease as the beam quality specifier $R_{50,D}$ increases, the exception to this being a value of $R_{50,D}$ of 1.23 cm where the calibration factor is much less than expected. This is unusual behaviour and this point is not consistent with the expected behaviour. McEwen (2001) did similar measurements of the absorbed dose to water calibration factor on a different Exradin A10 chamber and did not see this behaviour. These results are displayed in table B1 of the Appendix. All other calibration factors lie on an approximate straight line. There is no obvious constructional reason as to why the point at 1.23 cm deviates from the expected behaviour. It is possible that at this nominal beam energy the ionisation chamber was not positioned at the correct depth or there may have been instabilities in the output of the linear accelerator. The reason for the deviation is not understood. The validity of this point is suspected and as it appears to be an anomalous point it will not be included in any further analysis.

6.4 Polarity correction

The polarity corrections for each chamber are displayed in figure 14. It can be seen that the Advanced Markus chambers all show the same change in polarity correction with $R_{50,D}$. The magnitudes of the polarity corrections are all within 1% up to a value of $R_{50,D}$ of 3.48 cm. For the beam of $R_{50,D}$ of 1.23 cm, the polarity correction is as much as 2.5% for the Advanced Markus chamber, equivalent to a polarity effect of 5%. The polarity correction for the Exradin A10 chamber is also greatest here and this has a maximum value of 1.9%. The results for the Exradin A10 chamber are similar to those obtained by McEwen (2001), as displayed in table B2 of the Appendix.

There is nothing obvious in the design of either the Advanced Markus ionisation chamber or the Exradin A10 ionisation chamber to suggest why there should be such a large polarity correction. One cause of the polarity effect is charge storage in insulators and so these large polarity corrections could arise from charge being stored in the plastic behind the collector of the ionisation chamber. The size of the collector of the Advanced Markus chamber is bigger

than normal and so it is possible that this could be storing charge, which would lead to a larger polarity correction. However, the Exradin A10 chamber has a very small collector and so this does not explain the Exradin A10 polarity results.

The polarity correction is very sensitive to the measuring depth of the chamber in the water phantom and may change sign as a function of depth. If the depth was incorrect by only a fraction of a millimetre then this could have a significant effect on the polarity correction. This can be seen from the depth dose curve of figure 5. At low energies and hence low values of $R_{50,D}$, the dose deposited is changing rapidly with depth so any inaccuracy in positioning of chamber would cause an incorrect polarity correction to be measured. This is because there is a net deficit of negative charge close to the surface due to forward δ-ray transport. At depths close to and beyond the dose maximum there is a net excess of deficit charge due to primary electrons being stopped; the highest negative net charge occurs in the vicinity of the $R_{50,D}$ where most of the primary electrons are stopped (IPEM 2003).

6.5 Ion recombination

The recombination coefficients for all three Advanced Markus and Exradin A10 chambers are shown in table 5. Figure 15 shows a plot of the reciprocal of the standard to monitor ratio against the reciprocal of the polarising voltage for Advanced Markus chamber 0089 at a dose-rate of 5 Gy/min, which is equivalent to a dose-per-pulse of 0.035 cGy. It can be seen that there is a linear response of the reciprocal standard to monitor ratio against the reciprocal polarising voltage indicating that there is no significant deviation from the theory. This was the case for all four ionisation chambers at dose-rates of 2, 5 and 8 Gy/min; the points were more scattered from the linear response at a dose-rate of 1 Gy/min due to the small ionisation current at this dose-rate.

The coefficient c is a measure of the initial recombination and m is a function of the electric field strength, as given in equation (8). A table showing typical recombination coefficients for different parallel-plate chamber types is shown in table F1 in the Appendix.

For the Advanced Markus chambers it can be seen that there is some spread in the value of c between the three chambers, but in general the values are in good agreement with those of other chamber types. However, the gradient term, m, is of the order of 0.04, which is very different to that of the Classic Markus. This is most likely due to the change in design between these chamber types; the Classic Markus has a ‘top hat’ shaped electrode and it is known that due to this it does not have a uniform electric field. This could account for the much bigger value of m, as it is primarily a function of the electric field strength.

The Exradin A10 chamber has a gradient term, m, of 0.2548, which shows good agreement with that determined for another Exradin A10 chamber by McEwen (2001). It is also in good agreement with the gradient term of other parallel-plate chamber types. The constant term, c, for the Exradin A10 chamber was measured to be 1.0057. This is greater than the value of c for other parallel-plate chambers although it is not as large as that measured for a different Exradin A10 chamber by McEwen (2001).

A large value of the constant term, c, indicates a large value of the initial recombination. It is possible that this could arise due to flexing in the film window of the Exradin A10 ionisation

chamber. There may be an electrostatic force on the film window when the applied polarising voltage is changed. This could give an 'apparent' recombination correction as any flexing in the kapton window would change the size of the sensitive volume. A very non-linear plot of the type of figure 15 would also give rise to a large apparent initial recombination correction, but this was not the case for this particular chamber.

The recombination correction is not yet fully understood and some suggestions have been proposed to explain some of the unusual effects that can be seen. These include the suggestion that the chamber insulation may be behaving non-linearly as the voltage is increased, the geometry may change slightly as the field is increased, or even that there may be localised high fields in the chamber cavity that could affect recombination.

6.6 Perturbation correction

The ratio of the calibration factors at each energy for the Advanced Markus ionisation chambers and the Exradin A10 ionisation chamber to those of various NACP-02 and Roos ionisation chambers are displayed in figure 16.

The perturbation correction is exhibited through the energy dependence of the calibration factor. For an ionisation chamber with a zero perturbation correction the only energy dependence that would be seen in the calibration factor is due to the change in the stopping power ratio between water and air. As a result, two chambers with a zero perturbation will show a constant ratio in calibration factors at all energies. It can be seen that the Advanced Markus chambers follow the same general shape, which is reasonably flat with a variation of ± 0.7% about the flat response. There seems to be a residual non-zero perturbation in the response of the Exradin A10.

The perturbation correction is due to an air cavity effect and a chamber body effect. The large guard rings of both the Advanced Markus ionisation chamber and Exradin A10 ionisation chamber should mean that the air cavity perturbation is close to zero, so this effect may be due to backscatter from the ionisation chamber body.

6.7 Clinical results

The absorbed dose to water calibration factors determined at the NPL were used to predict what the calibration factors would be for a specific $R_{50,D}$ in the clinical beam at Norfolk and Norwich Hospital. The spread between the predicted absorbed dose to water calibration factors and those actually measured was determined. For the Advanced Markus chambers this spread was a maximum of 0.9% at a nominal beam energy of 9 MeV and for the Exradin A10 chamber was a maximum of 1.3% at a nominal beam energy of 16 MeV. Two independent ionisation chambers were taken to test: a PTW Roos chamber, serial number 0227, and a NACP-02 chamber, serial number DFA0006306. The Roos chamber had a maximum spread between the predicted and measured absorbed dose to water calibration factors of 1.9% while the NACP-02 chamber had a maximum spread of 0.3%.

The size of the spread between the predicted and measured absorbed dose to water calibration factors is larger than expected, particularly in the case of the Roos chamber. It is interesting

to note that the Advanced Markus ionisation chambers have a similar sized spread at each of the nominal beam energies investigated and that it is in the same direction. The discrepancy observed between the predicted and measured calibration factors could arise from the fit to the points that was used in the prediction; a linear was used as it appeared to be a reasonable fit to the data. The residuals were determined and this fit seemed reasonable. No calorimetry was performed with the NPL reference chambers in the clinic, the absorbed dose to graphite calibration factors and stopping power ratios were interpolated to the relevant $R_{50,D}$.

The polarity corrections associated with each ionisation chamber were also measured in the clinic. These results are displayed in figure 18 together with the polarity corrections that were measured at the NPL. It can be seen from the graph that the polarity corrections measured in the clinic differ from those measured at the NPL; the largest polarity correction that needed to be applied was 0.5% to the Exradin A10 ionisation chamber at a nominal clinical beam energy of 9 MeV.

7 CONCLUSION

The manufacturers' drawings and radiographs of one Exradin A10 and three Advanced Markus ionisation chambers indicated that both types represent an improvement on the Classic Markus design of ionisation chamber for reference dosimetry. In particular, both the Advanced Markus and Exradin A10 chambers have much wider guard rings which ensure that the effective point of measurement is not displaced from the inside of the front entrance window, and neither chamber design has a 'top hat' shaped electrode to cause a distorted electric field within the sensitive volume.

Check source measurements that were carried out on these chambers appeared to have an upward trend; further check source measurements must be performed on each chamber to investigate whether this trend would continue. Each chamber had a small sensitive volume and so may take longer to settle than a chamber with a greater sensitive volume. The check source measurements of figure 10 were performed after the chambers had been exposed to the strontium-90 radioactive source for 30 minutes. The continuous current measurements indicate that they may need to be left longer than this to settle in a continuous radiation source such as strontium-90. This may explain the presence of a trend in the results if the chambers had not settled.

The continuous current measurement carried out on the Exradin A10 chamber indicated a very large difference in reading while settling. The initial reading was 60% higher than the final settled reading and so it would be beneficial to repeat a continuous current measurement on this ionisation chamber to investigate whether this was an accurate indication of the settling of the Exradin A10 chamber.

The absorbed dose to water calibration factors for the Advanced Markus chambers showed a common dependence on $R_{50,D}$. The calibration factor for the Exradin A10 chamber at the lowest energy studied appeared to be anomalous. It would be useful to recalibrate each of these chambers to investigate the repeatability of the calibration factors.
There appears to be a large difference between the polarity correction measured in the NPL linear accelerator beam and that measured in the clinical beam. For parallel-plate chambers the polarity effect is a charge balance effect. It may depend on the energy of the beam, the

angular distribution of the incident radiation, the measuring depth and the field size. All of these factors were different in the clinical beam compared to the NPL beam.

It is desirable that any polarity effect be small; the large polarity effect observed at the lowest energy studied on all three Advanced Markus chambers may not be considered acceptable. The size of the uncertainty associated with such a large polarity effect would be likely to influence the overall uncertainty in the calibration factor. The large inconsistency in the polarity correction measured at the NPL compared to that at the clinic indicates that further measurements, particularly at the lower energies need to be performed.

Measurements have been completed to characterise the response of three Advanced Markus ionisation chambers, serial number 0087, 0088 and 0089, and also an Exradin A10 ionisation chamber, serial number XCO12744. These measurements have revealed some interesting effects that it has not been possible to fully explain. All measurements need to be repeated to investigate the reproducibility of the absorbed dose to water calibration factors and the relevant corrections. The polarity effect is very large; there is a change in chamber reading of typically 5% at the lower energy when changing from positive to negative polarity. The Exradin A10 chamber has a large initial recombination component and a non-zero perturbation correction is indicated from the chamber's energy response.

The response of three Advanced Markus ionisation chambers was determined and found to be similar and typical of this chamber type. Only one Exradin A10 chamber was available to test and so no conclusions can be drawn from these measurements whether this response is typical of the Exradin A10 chamber type.

From the measurements reported here, one would conclude that the Advanced Markus chamber is currently not suitable for reference dosimetry in electron beams due to the large polarity effect. Without measurements with more chambers of the Exradin A10 type it is not possible to determine whether the response observed is typical of the chamber type. Further measurements should be made before these chamber types could be recommended for use with the IPEM Code of Practice (IPEM 2003).

8 ACKNOWLEDGEMENTS

The author would like to thank Mr A DuSautoy and Mr R Thomas for their invaluable advice and assistance with the project and Dr M McEwen, formerly of NPL and now of NRC, Canada, for his many patient explanations over email. Thanks must also go to Mr C Thomas and Mr G Bostock for keeping the NPL linear accelerator online and stable.

Recognition must also be given to Dr A Williams and his colleagues of the Norfolk and Norwich Hospital for assistance and use of their facilities.

The author would also like to gratefully acknowledge the financial support of the UK Department of Trade and Industry (National Measurement System Policy Unit).

Thanks are due to PTW-Freiburg and their UK supplier Vertec Scientific for the loan of the three Advanced Markus chambers, and also to Standard Imaging Limited and Oncology Systems Limited for the loan of the Exradin A10 chamber.

9 REFERENCES

JW Boag and J Currant 1980 Current collection and ionic recombination in small cylindrical ionisation chambers exposed to pulsed radiation *Br. J. Radiol.* **53** 471-478

Burns D T, Duane S and McEwen M R 1995 A new method to determine ratios of electron stopping powers to an improved accuracy *Phys. Med. Biol.* **40** 733-739

Burns D T, Ding G X and Rogers D W O 1996 R50 as a beam quality specifier for selecting stopping power rations and reference depths for electron dosimetry *Med. Phys.* **23** 383

Burns D T and McEwen M R 1997 Ion recombination corrections for the NACP parallel-plate chamber in a pulsed electron beam *Phys. Med. Biol.* **43** 2033-2045

IAEA (International Atomic Energy Agency) 1996 The use of plane-parallel ionisation chambers in high-energy electron and photon beams. An international code of practice for dosimetry *Technical Report* 381 (Vienna: IAEA)

ICRU (International Commission on Radiation Units and measurements) 1992 Radiation Dosimetry: electron beams with energies between 1 and 50 MeV ICRU *Report* 35

IPEM (Institute of Physics and Engineering in Medicine) 2003 The IPEM code of practice for electron dosimetry for radiotherapy beams of initial energy from 4 to 25 MeV based on an absorbed dose to water calibration *Phys. Med. Biol.* **48** 2929-2970

IPEMB (Institute of Physics and Engineering in Medicine and Biology) 1996 The IPEMB code of practice for electron dosimetry for radiotherapy beams of initial energy from 2 to 50 MeV based on air kerma calibration *Phys. Med. Biol.* **41** 2557-2603

Klevenhagen S C 1985 *Physics of Electron Beam Therapy* Medical Physics Handbooks (Adam Hilger Ltd) 138-153

McEwen M R, DuSautoy A R and Williams A J 1998a The calibration of therapy level electron beam ionisation chambers in terms of absorbed dose to water *Phys. Med. Biol.* **43** 2503-2519

McEwen M R, Williams A J and DuSautoy A R 1998b Trial calibrations of therapy level electron beam ionisation chambers in terms of absorbed dose to water *NPL Report* CIRM 20

McEwen M R, Williams A J and DuSautoy A R 2001 Determination of absorbed dose calibration factors for therapy level electron beam ionisation chambers *Phys. Med. Biol.* **46** 741-755

McEwen M R 2001 *Private Communication*

Roos M, Derikum K and Krauss A 2000 Deviation of the effective point of measurement of the Markus chamber from the front surface of its air cavity in electron beams IAEA-TECDOC **1173** International Atomic Energy Agency, Wien 53-64

Williams A J, McEwen M R and DuSautoy A R 1998 A calculation of the water to graphite perturbation factor ratios for the NACP type 02 ionisation chamber using Monte Carlo techniques *NPL Report* CIRM 13

10 CHAMBER MANUFACTURERS AND SUPPLIERS

PTW-FREIBURG	Lörracher Strasse 7, D-79115 Freiburg, Germany
UK Supplier	VERTEC SCIENTIFIC Ltd 5 Comet House, Calleva Park, Aldermaston, Reading RG7 8JA
STANDARD IMAGING Inc.	7601 Murphy Drive, Middleton, WI 53562, USA
UK Supplier	ONCOLOGY SYSTEMS Ltd 11 Park Plaza, Battlefield Enterprise Park, Shrewsbury SY1 3AF

APPENDIX

Chamber dimensions	
front window thickness	≤ 1 mm
collecting electrode diameter	≤ 20 mm
ratio of guard width to cavity height	≥ 1.5
cavity height	≤ 2 mm
In-scattering perturbation, P_{cav}	< 1 %
Backscattering perturbation effect, P_{wall}	< 1 %
Polarity effect	< 1 %
Leakage current	$< 10^{-14}$ A
Long-term stability	± 0.5 %

Table A1. Preferred properties of a parallel-plate chamber in electron radiation (from IAEA 1996)

E_{nom} (MeV)	$R_{50,D}$ (cm)	$d_{ref,w}$ (cm)	$N_{u,w}$ (Gy/μC)
4	1.23	0.64	595.6
6	1.97	1.08	592.0
8	2.75	1.55	588.2
10	3.48	1.99	584.0
12	4.23	2.44	582.3
16	5.72	3.33	575.0

Table B1. Absorbed dose to water calibration factors for chamber A10-103 (from McEwen 2001)

E_{nom} (MeV)	$R_{50,D}$ (cm)	Correction to negative polarity
4	1.23	0.9850
6	1.97	0.9838
8	2.75	0.9869
10	3.48	0.9886
12	4.23	0.9909
16	5.72	0.9948

Table B2. Polarity corrections for Exradin A10 chamber 103 (from McEwen 2001)

E_{nom} (MeV)	$N_{ref,g}$ (Gy/μC)		
	N30-09	**N37-01**	**N37-02**
4	140.09	125.70	122.74
6	139.57	125.20	122.23
8	138.20	124.03	121.10
10	137.48	123.36	120.46
12	136.58	122.43	119.53
16	134.79	120.95	118.04
19	133.96	120.18	117.37

Table C1. Graphite calibration factors for NPL reference chambers (from McEwen *et al* 1998b)

E_{nom} (MeV)	$R_{50,D}$ (cm)	$s_{w/air}/s_{g/air}$
4	1.23	1.1466
6	1.97	1.1459
8	2.75	1.1452
10	3.48	1.1445
12	4.23	1.1437
16	5.72	1.1423
19	6.60	1.1412

Table D1. Stopping power ratio at the reference depth used for each energy (from McEwen *et al* 1998b)

Source of uncertainty	**Standard Uncertainty (± %)**	
	Type A	**Type B**
Graphite calibration factor for NPL chambers	-	0.35
Ratio of chamber measurements	0.1	-
Ratio of stopping powers	-	0.5
Ratio of perturbation factors	-	0.35
Recombination correction	0.17	-
Polarity correction	0.1	-
Electrometer calibration	-	0.05
Quadratic sum	0.22	0.71
Combined uncertainty	0.75	

Table E1. Uncertainties in the calibration of an ionisation chamber in terms of absorbed dose to water (from NPL calibration certificate for customer electron beam ionisation chamber 2003)

Chamber	***c***	***m***
NACP	1.0012	0.22
Roos	1.0014	0.16
Classic Markus	1.0022	0.20
Exradin A10 s/n 103	1.0077	0.259

Table F1. Recombination coefficients for different ionisation chamber types (from McEwen 2001)